

High-throughput free energies and water maps for drug discovery by molecular density functional theory

Sohvi Luukkonen

Maison de la Simulation, USR 3441 CNRS-CEA-Université Paris-Saclay, 91191 Gif-sur-Yvette, France

Luc Belloni

LIONS, NIMBE, CEA, CNRS, Université Paris-Saclay, 91191 Gif-sur-Yvette, France

Daniel Borgis

*Maison de la Simulation, USR 3441 CNRS-CEA-Université
Paris-Saclay, 91191 Gif-sur-Yvette, France and
PASTEUR, Département de chimie, École normale supérieure,
PSL University, Sorbonne Université, CNRS, 75005 Paris, France*

Maximilien Levesque

*PASTEUR, Département de chimie, École normale supérieure,
PSL University, Sorbonne Université, CNRS, 75005 Paris, France*

(Dated: August 18, 2021)

arXiv:1806.03118v1 [physics.chem-ph] 8 Jun 2018

Abstract

The hydration or binding free energy of a drug-like molecule is a key data for early stage drug discovery. Hundreds of thousands of evaluations are needed, which rules out the exhaustive use of atomistic simulations and free energy methods. Instead, the current docking and screening processes are today relying on numerically efficient scoring functions that lose much of the atomic scale information and hence remain error-prone. In this article, we show how a probabilistic description of molecular liquids as implemented in the molecular density functional theory predicts hydration free energies of a state-of-the-art benchmark of small drug-like molecules within 0.5 kJ/mol (0.1 kcal/mol) of atomistic simulations, along with water and polarization maps, for a computation time compatible with screening and docking.

I. INTRODUCTION

The development of a new drug is a long and expensive process, consuming in average 10 to 12 years and between 2.5 and 3.0 billion dollars [1]. Structure-based drug design process starts with the identification of a protein related to the disease, called the target, whose activity needs to be modulated with the drug to be found. Once the target is found, the early stages of drug discovery consist in finding few potential drug leads via back and forth between *in silico* methods that start from databases of millions of small drug-like molecules. The screening, i.e., ranking, of drug candidates is then done by a score, mimicking the binding free energy between the small ligand molecule and the protein when the ligand is docked in the active site of the protein.

However, computing free energies of a process such as binding or solvation is difficult as it requires the sampling of all possible states that could be visited during the transformation. Nevertheless, free energy methods that use alchemical transformations exist. They range from simple exponential averaging (EXP) introduced by Zwanzig [2] 60 years ago to more sophisticated method employing non-physical intermediate states such as the thermodynamic integration (TI) [3], free energy superposition, the Bennett acceptance ratio (BAR) [4], the weighted histogram analysis method (WHAM) [5] or the multistate Bennett acceptance ratio (MBAR) [6]. All these methods require multiple ergodic molecular dynamics (MD) or Monte-Carlo (MC) simulations for a single free energy estimate. In other words, they require multiple simulations to be run, typically few tens, eventually in parallel, with the associated few tens of simulation time. These methods and the protocol associated for producing the free energy estimate defines today's standard in terms of free energy predictions.

In the case of drug discovery, binding free energies need to be calculated in water as the protein-ligand interaction often takes place in an aqueous environment. The direct calculation of binding free energies

in the solvent is thus especially difficult because all the configurations of the solvent molecules have to be sampled in addition to protein and ligand configurations. However the binding free energy between two molecules A and B in solution can be rigorously expressed in terms of the solvation free energies of the complex AB, the molecule A, the molecule B and of the binding free energy in vacuum :

$$\Delta G_{\text{bind,solv}}^{\text{AB}} = \Delta G_{\text{solv}}^{\text{AB}} - (\Delta G_{\text{solv}}^{\text{A}} + \Delta G_{\text{solv}}^{\text{B}}) + \Delta G_{\text{bind,vac}}^{\text{AB}}. \quad (1)$$

Since the binding in vacuum, $\Delta G_{\text{bind,vac}}^{\text{AB}}$, is much easier to compute, the difficulty in obtaining a binding free energy in solution is moved to the solvation free energy calculation (SFE), that is, in ΔG_{solv} of equation 1. SFE calculations can be done with explicit or implicit models of water. The theory behind alchemical transformations is exact, thus the only approximations are the choice of a force field for describing the interaction the solute-solvent interaction and numerical errors. However, in explicit solvent alchemical transformations are computationally expensive as multiple ergodic simulations are needed to accumulate enough uncorrelated data points to have an acceptable statistical error. Obtaining a single solvation free energy of a small drug-like molecule requires hundreds cpu.h with an explicit solvent method, which is too slow for the screening of millions of drug-like ligands of the early stage *in silico* drug discovery process. Hence they can only be used in “late-stage” *in silico* drug design. Therefore, one uses parameterized implicit solvent models or scoring functions for the initial stages of the screening process. Implicit solvent alchemical transformations estimate SFEs in few tens of seconds at most. Scoring functions are fast, more or less empirical functions that use some molecular descriptors of the ligands to rank them [7]. These highly parameterized functions are fast enough for processing large databases, requiring few minutes at most per score [8]. In some cases, they work really well, but the lack of physical support and insight was shown by recent reviews to lead to unpredictable qualities [9, 10].

Alternative so called “end-point” methods exist, ie. methods without alchemical intermediates, such as Watermap [11, 12] where the water-density is obtained from an explicit solvent MD simulation and is then injected into a functional that estimates the binding free energy. Some other methods are based solely on electrostatics such as AquaSol [13], which uses a dipolar Poisson–Boltzmann–Langevin formalism to calculate the solvent density and solvation free energy.

Other “end-point” approaches have roots in the liquid state theories. They are based on the Ornstein-Zernike equation (OZ) solved within the integral equation or classical density function theory (cDFT) formalism. Among them, reference interaction site model (RISM) and 3D-RISM [14–19] are simplified versions which ignore the full molecular description of the solvent and replace it by site-site correlations only. They enable the calculation of the site densities, such as the water-oxygen or hydrogen densities and of the solvation free energy by minimizing a site-functional [20] or solving the 3D-RISM equations. These methods are having large success and are gaining momentum because of their good balance

between precision, simplicity and speed. Nevertheless, they rely on simplifying molecules to a set of sites correlated together, not on a full molecular description and hence they use multiple compromises with purely phenomenological corrections.

On the other hand, the molecular density functional theory (MDFT) [21–26] and molecular integral equation theory (MIET) are the only methods based on liquid state theories that keep the full molecular picture by solving the molecular Ornstein-Zernike equation (MOZ). It is diagrammatically consistent. Since Ding et al. [27], MDFT can be solved efficiently and rigorously at the hypernetted chain (HNC) level of approximation. In this paper, we assess of MDFT in the HNC approximation (MDFT-HNC) to predict solvation free energies of small drug-like molecules. MDFT-HNC is a rigorous, lowest level of the hierarchy of functionals for the MDFT: It can thus be used as a starting point to be systematically improved. While this can be done by developing so-called bridge functionals [20, 28–32], this paper is dedicated to MDFT-HNC in its “crudest” approximation and its capacity to predict solvation free energies of small drug-like molecules. It lays the foundations of the future of MDFT for the early stage *in silico* drug discovery.

In section II, we describe the MDFT framework. In section III, we present reference calculations using state-of-the-art alchemical transformations. In section IV, we compare the references to MDFT-HNC for what concerns solvation free energies and solvation structure of drug-like molecules. Conclusions and perspectives are drawn in section V.

II. MOLECULAR DENSITY FUNCTIONAL THEORY

The molecular density functional theory of classical, molecular fluids, computes rigorously and efficiently the solvation free energy and equilibrium solvent density around a solute. MDFT is a cousin of the well-known Kohn-Sham density functional theory for electrons, extended to finite temperature in the grand canonical ensemble by Mermin [33–35]. In the classical density functional theory formalism, the solvation free energy ΔG_{solv} (SFE) is defined as the difference between the grand potential Ω of the solvated system, with the grand potential Ω_b of the bulk solvent:

$$\Delta G_{\text{solv}} = \Omega - \Omega_b = \min \{ \mathcal{F}[\rho] \} = \mathcal{F}[\rho_{\text{eq}}], \quad (2)$$

where $\mathcal{F}[\rho]$ is the functional to be minimized, $\rho = \rho(\mathbf{r}, \omega)$ the molecular solvent density function with \mathbf{r} a three dimensional vector and ω the Euler angles (θ, ϕ, ψ) , characterizing the position and the orientation of the rigid solvent molecule, typically the TIP3P model for water [36] and ρ_{eq} is the equilibrium solvent density.

The MDFT functional \mathcal{F} , to be minimized, is made of three parts:

$$\mathcal{F} = \mathcal{F}_{\text{id}} + \mathcal{F}_{\text{ext}} + \mathcal{F}_{\text{exc}}, \quad (3)$$

where \mathcal{F}_{id} is the ideal term of a fluid of non-interacting particles, \mathcal{F}_{ext} is the external term induced by the solute (the protein, ligand or complex embedded in water), and \mathcal{F}_{exc} is the excess term that includes structural correlations between solvent molecules. The ideal term, coming solely from the entropy of mixing of the solvent molecules, reads

$$\mathcal{F}_{\text{id}} = k_{\text{B}}T \int d\mathbf{r}d\omega \left[\rho(\mathbf{r}, \omega) \ln \left(\frac{\rho(\mathbf{r}, \omega)}{\rho_{\text{bulk}}} \right) - \Delta\rho(\mathbf{r}, \omega) \right], \quad (4)$$

where $k_{\text{B}}T$ is the thermal energy, $d\mathbf{r} \equiv dx dy dz$, $d\omega \equiv d\cos\theta d\phi d\psi$ and $\Delta\rho(\mathbf{r}, \omega) \equiv \rho(\mathbf{r}, \omega) - \rho_{\text{bulk}}$ is the excess density over the bulk homogeneous density $\rho_{\text{bulk}} \equiv n_{\text{bulk}}/8\pi^2$. n_{bulk} is typically 0.033 molecule per \AA^3 for water at room conditions ($\equiv 1 \text{ kg/L}$). $8\pi^2$ is the angular normalization constant. The external contribution comes from the interaction potential v_{ext} between the solute molecule and a solvent molecule. It reads

$$\mathcal{F}_{\text{ext}} = \int d\mathbf{r}d\omega \rho(\mathbf{r}, \omega) v_{\text{ext}}(\mathbf{r}, \omega), \quad (5)$$

where v_{ext} is the interaction energy between a solute and a solvent molecule that is made of a van-der-Waals term, typically Lennard-Jones, and electrostatic interactions. Those are the same non-bonded force field parameters as in a molecular dynamics simulation. For now and in what follows, the MDFT does not use the intramolecular force field parameters as the solute and the solvent are considered rigid for the sake of the simplicity of the demonstration. For the solvent, we use the TIP3P [36] water model as it is the most commonly found in drug design applications and thus in reference simulations detailed below. The final, excess term describes the effective solvent-solvent interactions, may be written as a density expansion around the homogeneous bulk density ρ_{bulk} :

$$\begin{aligned} \mathcal{F}_{\text{exc}} &= -\frac{k_{\text{B}}T}{2} \int d\mathbf{r}_1 d\omega_1 \int d\mathbf{r}_2 d\omega_2 \Delta\rho(\mathbf{r}_1, \omega_1) c^{(2)}(\mathbf{r}_{12}, \omega_1, \omega_2) \Delta\rho_2(\mathbf{r}_2, \omega_2) + \mathcal{F}_{\text{b}} \\ &= -\frac{k_{\text{B}}T}{2} \int d\mathbf{r}_1 d\omega_1 \Delta\rho(\mathbf{r}_1, \omega_1) \gamma(\mathbf{r}_1, \omega_1) + \mathcal{F}_{\text{b}} \\ &= \mathcal{F}_{\text{HNC}} + \mathcal{F}_{\text{b}}, \end{aligned} \quad (6)$$

where $c^{(2)}(\mathbf{r}_{12}, \omega_1, \omega_2)$ is the homogeneous solvent-solvent molecular direct correlation function, \mathcal{F}_{b} the bridge functional and $\gamma \equiv c^{(2)} * \Delta\rho$ is the indirect solute-solvent correlation defined as the spatial and angular convolution of the excess density with the direct correlation function. If one cuts the expansion to order two in excess density, that is, if one cancels the bridge functional [37], one finds that the MDFT

functional produces at its variational minimum the well-known HNC relation for the solute-solvent distribution function:

$$g(\mathbf{r}, \omega) = \frac{\rho_{\text{eq}}(\mathbf{r}, \omega)}{\rho_{\text{bulk}}} = e^{-\beta v_{\text{ext}}(\mathbf{r}, \omega) + \gamma}, \quad (7)$$

where $\beta \equiv \frac{1}{k_B T}$. Therefore, we call the first term of the excess functional the HNC functional. The function $c^{(2)}$ of the bulk solvent for a given temperature and pressure is an input in the present theory and is provided by previous Monte Carlo simulations coupled to integral equations calculations [38, 39] carefully corrected for finite-size effects [40]. Higher-order correlation functions could be computed but usually are not numerically feasible. The rest of the excess term, the so-called bridge functional can be approximated rigorously or empirically [28–30]. However in this paper we benchmark MDFT as a prospective tool for drug design applications, at its lowest level of accuracy : the MDFT-HNC, *i.e.* without a bridge functional. This HNC level can only be improved by adding bridge functionals. Contrary to other liquid state theories, the MDFT-HNC is a rigorous basis one can only improve.

This theory and corresponding algorithms are implemented into a in-house high performance code that predicts a hydration free energy in few seconds to minutes. It depends on the simulation cell size and spacial and angular resolutions [27]. The MDFT code includes, as expected, partial molar volume correction (also called PC or ISc correction) to the solvation free energy [41, 42].

III. REFERENCE CALCULATIONS FROM SIMULATION

To assess the quality of the hydration free energies (HFE) predicated in few minutes by MDFT-HNC, we use the FreeSolv database [43, 44]. FreeSolv concatenates hydration free energies of 642 neutral drug-like molecules, as measured experimentally and calculated with state-of-the-art MBAR from explicit solvent molecular dynamics simulations with the Generalized Amber force field (GAFF) [45] version 1.7 with AM1-BCC partial charges [46, 47] and TIP3P model [36] of water. In these simulations, the solute is flexible, that is, its internal degrees of freedom are free. How the hydration free energy depends on the ensemble of conformers for a given molecule is a statistical mechanical problem in itself, already tackled for instance through the exploration of so-called end-point calculations. The illustration of this is given in fig. 1, where one sees HFEs of all FreeSolv molecules as calculated with a flexible solute, *i.e.*, with a mixture of solute conformers, and as calculated for a rigid solute, that is, for a single solute conformer. We used the initial conformations given in FreeSolv database. As summarized in Table I, the mean unsigned error with respect to experimental changes from 4.3 kJ/mol to 5.4 kJ/mol because of the single point calculation and the Pearson R coefficient, that is the correlation, change from 0.94 to

0.89. It is not the point of this manuscript to review those methods to take into account the flexibility or mix of conformers. For the sake of the simplicity of the demonstration, we performed rigid solute (a single conformer) insertion/destruction Monte Carlo (MC) simulations of all molecules in the databases coupled with the Bennett acceptance ration (BAR) analysis [4, 39, 40, 48]. Simulations details can be found in the supplementary information (SI). Since we use the same force fields and conformers in the simulations and in MDFT, i.e., since we lie in the same force field approximation, the fully atomistic simulation based alchemical transformation calculations can be considered as reference calculations. The computation cost of such a reference state-of-the-art simulation is of the order of one day or few hours with the most recent GPU compatible codes.

Additionally, we performed implicit solvent calculations with Yank (an open source Replica Exchange MC code for alchemical transformation [6, 49–55]) on the whole FreeSolv database. In the implicit solvent calculations the rigid solute is also described with GAFF, while the implicit solvent is of type GB-OBC(II) [56]. The simulation details are given in SI. Knight and Brooks have published a review of implicit solvent models for a previous version of the FreeSolv database [57]. Our calculations are much more limited than Knight and Brooks as we only seek to illustrate typical results, but our conclusions are in full agreement with theirs.

We also evaluated the capacity of MDFT to predict the equilibrium solvent structures around a solute, the so-called *water maps*. To this end, we performed reference simulations of a rigid solute in water chosen to be representative of the molecules of the FreeSolv database : the quinoline (C₉H₇N). It has the correct average size, contains a hetero-atom and a cycle.

IV. MOLECULAR DENSITY FUNCTIONAL THEORY CALCULATIONS

A. Hydration free energy

Here we assess the quality of hydration free energies of small drug-like molecules predicted by MDFT-HNC. In fig. 1, we show the correlation between the experimental HFE of the FreeSolv database as compared to those obtained by a MDFT-HNC calculations. The results, that is, the output of the minimization of the functional given in eq. 2, were obtained within a cubic supercell of side 32 Å, with periodic boundary conditions, a spacial resolution of 0.25 Å (= 128 grid nodes in each direction) and an angular resolution of 84 orientations per spatial grid node. The MDFT calculations were performed on the initial configuration given in the FreeSolv database. MDFT calculations did not converge for 36 molecules (5 % of the database, see SI for a list of these molecules) that have a local charge too high for the HNC approximation (see SI for more information). All results presented below are for the 606

molecules that led to convergence.

In fig. 1, we show the correlations between experimental HFE, reference calculations in explicit and implicit solvents, and those predicted by MDFT-HNC. Table I concatenates the statistical measures characterizing those four correlations.

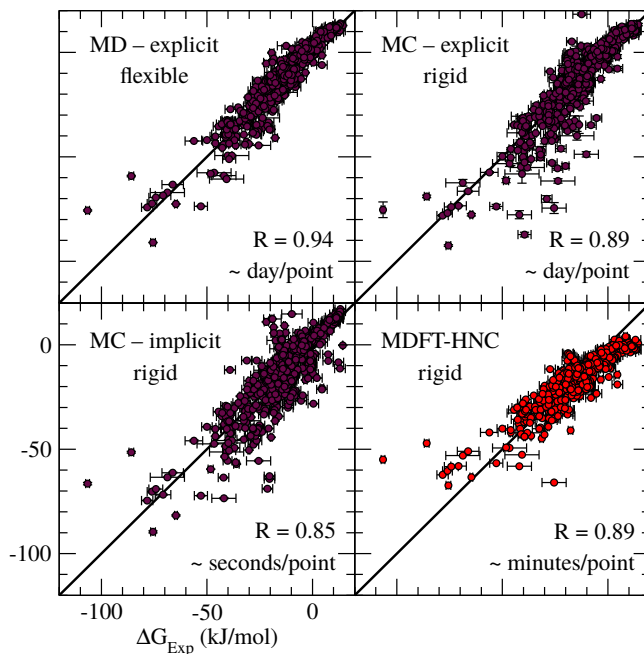


Figure 1. Correlations between experimental hydration free energies and hydration free energies obtained with (i) a flexible solute in explicit solvent alchemical transformation simulations and with a rigid solute (ii) in explicit solvent simulations, (iii) in implicit solvent simulations and (iv) with MDFT-HNC calculations for the FreeSolv database.

MDFT-HNC has a mean unsigned error (MUE) to experimental values of 5.9 kJ/mol, while reference simulations MUE equals 5.4 kJ/mol. HFEs are in all cases well (linearly and monotonically) correlated as can be seen in fig. 1 and confirmed with Pearson’s R and Spearman’s ρ coefficients close to 0.9. The computational cost, or average computation time, for each MDFT SFE lies within 5 minutes on a single cpu thread. The current implementation of MDFT uses shared memory parallelism to decrease this time to less than 1 minute on any 2018’s laptop that has 4 to 8 available threads. This is 3 orders of magnitude faster than reference calculations, for a MUE increased by 0.5 kJ/mol.

While taking few tens of seconds at most to predict SFE, parametric implicit solvent simulations have a MUE of 6.8 kJ/mol, i.e. an increase of 0.9 kJ/mol when compared with MDFT-HNC, and correlation constants below 0.9. These results agree well with the deep review by Knight and Brooks [57]. Furthermore, it should be noted that MDFT also gives the full molecular equilibrium solvent structure around the solute, as shown in the next section, that can not be obtained with implicit solvent

	Flexible solute ^(a)		Rigid solute	
	Explicit solvent	Explicit solvent	Implicit solvent	MDFT HNC
MUE (kJ/mol)	4.3	5.4	6.8	5.9
RMSE (kJ/mol)	5.8	8.3	9.5	7.5
P-bias (%)	-11.5	-3.2	-5.9	15.0
Pearson’s R	0.94	0.89	0.85	0.89
Spearman’s ρ	0.94	0.90	0.83	0.88
Kendall’s τ	0.80	0.75	0.67	0.70
cpu-time (s)	$\sim 10^5$	$\sim 10^5$	$\sim 10^0$	$\sim 10^2$ ^(b)

Table I. Summary of statistical measures characterizing the correlation between the experimental hydration free energies and the ones obtained from (i) flexible solute \equiv a mixture of conformers in explicit solvent molecular dynamics simulations, and (ii) from rigid solute \equiv single conformer calculation in reference explicit solvent Monte Carlo simulations, or (iii) implicit solvent MC simulations and (iv) MDFT-HNC, for the whole FreeSolv database. Cross-correlations between computational methods are given in SI. Statistical measures : MUE - mean unsigned error, RMSE - root-mean-squared error, P-bias - percent bias, Pearson’s correlation coefficient R (measure of linear correlation), Spearman’s and Kendall’s ranking correlation coefficients ρ and τ (measures of monotonic correlation). Orders of magnitude of cpu-times are given per solute molecule. One can do thousands of MDFT or implicit solvent calculations, not contrary to explicit solvent calculations. (a) Simulations done by Mobley *et al.* [43] (b) Distribution of computing time is given in SI.

MD simulations where the density is homogeneous everywhere outside the solute core.

In summary, MDFT-HNC trades 0.12 kcal/mol of precision compared to reference fully atomic simulations for a speed up of 3 orders of magnitude at least. It takes less than an hour to compute HFEs for the whole Freesolv database by MDFT-HNC. It is quick enough to be used in virtual screening of millions of molecules which is not the case of explicit solvent simulations and a large potential improvement with respect to the methods, implicit solvent and scoring functions, used in drug discovery. At the moment the virtual screening is a multistage process with an initial screening stages with scoring functions to select ~ 100 hits and a final screening with MD simulations to obtain few final leads. This multistage process could be replaced with a unique MDFT-based stage.

B. Solvent equilibrium structure, polarization and beyond

Equation 2 states that at the same time as MDFT produces the solvation free energy of arbitrarily complex molecule (the value of the functional at its minimum), it produces the equilibrium solvent structure around this solute (the density that minimizes the functional), in its full molecular description, $g(\mathbf{r}, \omega) = \frac{\rho(\mathbf{r}, \omega)}{\rho_{\text{bulk}}}$. From this full molecular distribution, one can extract more readable information. For instance, the first moment of $g(\mathbf{r}, \omega)$ is the three dimensional scalar field $g(\mathbf{r}) \equiv \frac{1}{8\pi^2} \int g(\mathbf{r}, \omega) d\omega$ from which one can derive the usual spherically symmetric radial distribution function $g_i(r)$ between solute sites and water oxygens. Fig. 2(a) shows the three dimensional scalar field $g(\mathbf{r})$ in the plane of the quinoline molecule and fig. 3 shows the radial distribution functions between the heavy atoms of quinoline and solvent oxygen atoms. Fig. 3 also shows the radial distribution functions obtained from a explicit solvent simulation.

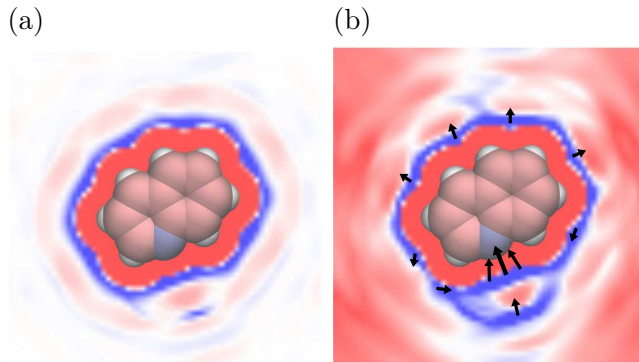


Figure 2. (a) Water density map (red : $\rho < \rho_{\text{bulk}}$, white : $\rho = \rho_{\text{bulk}}$ and blue : $\rho > \rho_{\text{bulk}}$) and (b) norm of the polarization vector field (blue : high polarization, black arrows representing the orientation) in the plane of the quinoline molecule obtained with MDFT-HNC

We see the solvation layer structure in fig. 2(a) and radial distribution functions, fig. 3 given by the MDFT-HNC corresponds well with the ones obtained with simulation : The first peak of the rdfs are at the right distance, meaning that the first solvation shell lies where it should. We observe a classical overestimation with HNC of the height of the first peak. The $g(r)$ for nitrogen-oxygen is qualitative only: The nitrogen atom wears a high partial charge of $-0.65e$, which is difficult a case for HNC that does not perform as well on strong charges. The typical overestimation of the height of the first peak in the HNC approximation is due to the theory being a second order density expansion of the functional, missing higher order repulsion terms (packing effects) between excess densities [28].

Another important quantity embedded in $g(\mathbf{r}, \omega)$ is the polarization field $\mathbf{P}(\mathbf{r}) \equiv \int \hat{\omega} g(\mathbf{r}, \omega) d\omega$ where $\hat{\omega}$ is the unitary vector along the dipole axis depending on (θ, ϕ) only. Fig. 2(b) shows the l_2 -norm of

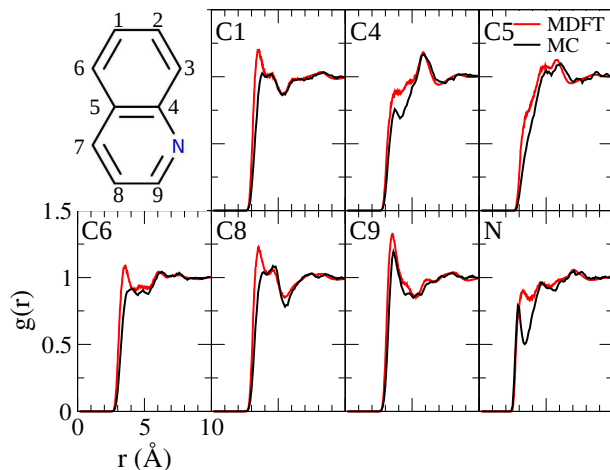


Figure 3. Chemical structure of the quinoline and the radial distribution function $g(r)$ between the heavy atoms of the quinoline and water oxygens (red lines correspond to MDFT-HNC as obtained in few minutes, and black ones to MD simulations as obtained in few hours).

the polarization field, i.e., $\|\mathbf{P}(\mathbf{r})\|$, in the plane of the quinoline molecule obtained with MDFT-HNC. As expected we find high polarization close to the sites wearing localized charges, and the expected polarization with OH pointing toward N. One can also obtain so called water maps from $g(\mathbf{r}, \omega)$, catching the most probable water molecules position and orientation around the solute. Fig. 4 shows the four most probable position and the orientation of water molecules around the quinoline molecules. They are found close to the nitrogen atom.

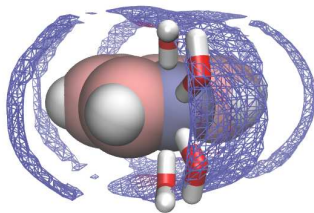


Figure 4. Representation of the quinoline molecule with four most probable water molecules and the isosurface corresponding to $\rho = 3\rho_{\text{bulk}}$.

It should be noted that the equilibrium molecular solvent density $g(\mathbf{r}, \omega)$ is a direct output of MDFT. In the case of molecular simulations, one would have to accumulate such data during a long trajectory, averaging in a three-dimensional pixel (a voxel), typically of width 0.5 \AA . This can be tackled nowadays, especially with the recent approach using also the forces to decrease the variance of the estimate of g [58, 59]. Nevertheless, accumulating data for a given orientation in the full six-dimensional orientation and position space is a daunting task, even more difficult than computing SFE. MDFT produces this

6-dimensional map in the same few minutes as it needs to predict the SFE.

V. CONCLUSION

The hydration or binding free energy of a drug-like molecule is a key data for early stage drug discovery. This quantity is nowadays calculated either (i) by fast but inaccurate scoring functions or implicit solvent methods, or (ii) by accurate but slow atomistic simulations and free energy methods. In this paper, we have shown on the 600+ drug-like molecules of the FreeSolv database that the molecular density functional theory (MDFT) in its simplest hypernetted-chain (HNC) approximation is able to trade 0.5 kJ/mol (0.1 kcal/mol) of mean unsigned error compared to the most precise simulation for a speed up of five orders of magnitude for the solvation free energies. MDFT can thus be used directly during the screening and docking process. Furthermore, since MDFT-HNC is exact up to second order in density correlations, it can only be improved by bridge functionals. Last but not least, the MDFT also predicts the full molecular, angular, three-dimensional solvent density, also called water maps, around the solute or protein-ligand complexes, spotting where are the most important water molecules.

-
- [1] J. A. DiMasi, H. G. Grabowski, and R. W. Hansen. Innovation in the pharmaceutical industry: New estimates of R and D costs. *J. Health Eco.*, 47:20 – 33, 2016.
 - [2] R. W. Zwanzig. High temperature equation of state by a perturbation method. I. Nonpolar gases. *J. Chem. Phys.*, 22:1420–1426, 1954.
 - [3] J. G. Kirkwood. Statistical mechanics of fluid mixtures. *J. Chem. Phys.*, 3:300–313, 1935.
 - [4] C. H. Bennett. Efficient estimation of free energy differences from Monte Carlo data. *J. Comput. Phys.*, 22:245–268, 1976.
 - [5] S. Kumar, J. M. Rosenberg, D. Bouzida, R. H. Swendsen, and P. A. Kollman. The weighted histogram analysis method for free-energy calculations on biomolecules. I. The method. *J. Comput. Chem.*, 13(8):1011–1021, 1992.
 - [6] M. R. Shirts and J. D. Chodera. Statistically optimal analysis of samples from multiple equilibrium states. *J. Chem. Phys.*, 129(12):124105, 2008.
 - [7] D. B. Kitchen, H. Decornez, J. R. Furr, and J. Bajorath. Docking and scoring in virtual screening for drug discovery: methods and applications. *Nat. Rev. Drug Discov.*, 3:935–949, 2004.
 - [8] Z. Zhou, A. K. Felts, R. A. Friesner, and R. M. Levy. Comparative performance of several flexible docking programs and scoring functions: Enrichment studies for a diverse set of pharmaceutically relevant targets.

- J. Chem. Inf. Model.*, 47(4):1599–1608, 2007.
- [9] L. Chaput and L. Mouawad. Efficient conformational sampling and weak scoring in docking programs? Strategy of the wisdom of crowds. *J. Cheminformatics*, 9(1):37, 2017.
- [10] L. Chaput, J. Martinez-Sanz, N. Saettel, and L. Mouawad. Benchmark of four popular virtual screening programs: construction of the active/decoy dataset remains a major determinant of measured performance. *J. Cheminformatics*, 8(1):56, 2016.
- [11] R. Abel, T. Young, R. Farid, B. J. Berne, and R. A. Friesner. Role of the active-site solvent in the thermodynamics of factor xa ligand binding. *J. Am. Chem. Soc.*, 130(9):2817–2831, 2008.
- [12] T. Young, R. Abel, B. Kim, B. J. Berne, and R. A. Friesner. Motifs for molecular recognition exploiting hydrophobic enclosure in protein–ligand binding. *P. Natl. A. Sci.*, 104(3):808–813, 2007.
- [13] P. Koehl and M. Delarue. AquaSol: An efficient solver for the dipolar Poisson-Boltzmann-Langevin equation. *J. Chem. Phys.*, 132(6):064101, 2010.
- [14] D. Chandler and H. C. Andersen. Optimized cluster expansions for classical fluids. II. Theory of molecular liquids. *J. Chem. Phys.*, 57:1930–1937, 1972.
- [15] F. Hirata and P. J. Rossky. An extended RISM equation for molecular polar fluids. *Chem. Phys. Lett.*, 83(2):329–334, 1981.
- [16] D. Beglov and B. Roux. An integral equation to describe the solvation of polar molecules in liquid water. *The Journal of Physical Chemistry B*, 101:7821, 1997.
- [17] A. Kovalenko and F. Hirata. Three-dimensional density profiles of water in contact with a solute of arbitrary shape; a RISM approach. *Chemical Physics Letters*, 290:237, 1998.
- [18] A. Kovalenko and F. Hirata. Hydration free energy of hydrophobic solutes studied by a reference interaction site model with a repulsive bridge correction and a thermodynamic perturbation method. *J. Chem. Phys.*, 113:2793–2805, 2000.
- [19] A. Kovalenko and F. Hirata. Potential of mean force between two molecular ions in a polar molecular solvent: A study by the three-dimensional reference interaction site model. *J. Phys. Chem. B*, 103:7942–7957, 1999.
- [20] Y. Liu, S. Zhao, and J. Wu. A site density functional theory for water: Application to solvation of amino acid side chains. *J. Chem. Theory Comput.*, 9:1896–1908, 2013.
- [21] R. Ramirez, M. Mareschal, and D. Borgis. Direct correlation functions and the density functional theory of polar solvents. *Chemical Physics*, 319:261, 2005.
- [22] L. Gendre, R. Ramirez, and D. Borgis. Classical density functional theory of solvation in molecular solvents: Angular grid implementation. *Chem. Phys. Lett.*, 474:366–370, 2009.

- [23] D. Chandler, J. D. McCoy, and S-J. Singer. Density functional theory of nonuniform polyatomic systems. I. General formulation. *J. Chem. Phys.*, 85:5971, 1986.
- [24] D. Chandler, J. D. McCoy, and S. J. Singer. Density functional theory of nonuniform polyatomic systems. II. Rational closures for integral equations. *J. Chem. Phys.*, 85:5977, 1986.
- [25] R. Ramirez, R. Gebauer, M. Mareschal, and D. Borgis. Density functional theory of solvation in a polar solvent: Extracting the functional from homogeneous solvent simulations. *Phys. Rev. E*, 66:031206–031206–8, 2002.
- [26] S. Zhao, R. Ramirez, R. Vuilleumier, and D. Borgis. Molecular density functional theory of solvation: From polar solvents to water. *J. Chem. Phys.*, 134:194102, 2011.
- [27] L. Ding, M. Levesque, D. Borgis, and L. Belloni. Efficient molecular density functional theory using generalized spherical harmonics expansions. *J. Chem. Phys.*, 147(9):094107, 2017.
- [28] M. Levesque, R. Vuilleumier, and D. Borgis. Scalar fundamental measure theory for hard spheres in three dimensions. application to hydrophobic solvation. *The Journal of Chemical Physics*, 137:034115, 2012.
- [29] G. Jeanmairet, M. Levesque, V. Sergiievskiy, and D. Borgis. Molecular density functional theory for water with liquid-gas coexistence and correct pressure. *J. Chem. Phys.*, 142:154112, 2015.
- [30] C. Cageat, D. Borgis, and M. Levesque. Bridge functional for the molecular density functional theory with consistent pressure and surface tension. 2018.
- [31] S. Zhao, Z. Jin, and J. Wu. New theoretical method for rapid prediction of solvation free energy in water. *Journal of Physical Chemistry B*, 115:6971, 2011.
- [32] S. Zhao, Z. Jin, and J. Wu. Corrections to new theoretical method for rapid prediction of solvation free energy in water. *Journal of Physical Chemistry B*, 115:15445, 2011.
- [33] P. Hohenberg and W. Kohn. Inhomogeneous electron gas. *Phys. Rev.*, 136:B864, 1964.
- [34] W. Kohn and L. J. Sham. Self-consistent equations including exchange and correlation effects. *Phys. Rev.*, 140:A1133, 1965.
- [35] N. D. Mermin. Thermal properties of the inhomogeneous electron gas. *Phys. Rev.*, 137:A1441–A1443, 1965.
- [36] W. L. Jorgensen, J. Chandrasekhar, J. D. Madura, and M. L. Klein. Comparison of simple potential functions for simulating liquid water. *J. Chem. Phys.*, 79:926–935, 1983.
- [37] J.M.J. van Leeuwen, J. Groeneveld, and J. de Boer. New method for the calculation of the pair correlation function. I. *Physica*, 25(7):792 – 808, 1959.
- [38] J. Puibasset and L. Belloni. Bridge function for the dipolar fluid from simulation. *J. Chem. Phys.*, 136:154503, 2012.

- [39] L. Belloni. Exact molecular direct, cavity, and bridge functions in water system. *The Journal of Chemical Physics*, 147(16):164121, 2017.
- [40] L. Belloni and J. Puibasset. Finite-size corrections in simulation of dipolar fluids. *The Journal of Chemical Physics*, 147(22):224110, 2017.
- [41] V. Sergiievskiy, G. Jeanmairet, M. Levesque, and D. Borgis. Solvation free-energy pressure corrections in the three dimensional reference interaction site model. *J. Chem. Phys.*, 143:184116, 2015.
- [42] Volodymyr P. Sergiievskiy, Guillaume Jeanmairet, Maximilien Levesque, and Daniel Borgis. Fast computation of solvation free energies with molecular density functional theory: Thermodynamic-ensemble partial molar volume corrections. *J. Phys. Chem. Lett.*, 5:1935–1942, 2014.
- [43] D. L. Mobley. Experimental and calculated small molecule hydration free energies. UC Irvine: Department of Pharmaceutical Sciences, UCI., 2013.
- [44] G. D. R. Matos, D. Y. Kyu, H. H. Loeffler, John D. C., M. R. Shirts, and D. L. Mobley. Approaches for calculating solvation free energies and enthalpies demonstrated with an update of the FreeSolv database. *J. Chem. Eng. Data*, 62(5):1559–1569, 2017.
- [45] J. Wang, R. M. Wolf, J. W. Caldwell, P. A. Kollman, and D. A. Case. Development and testing of a general AMBER force field. *J. Comput. Chem.*, 25(9):1157–1174, 2004.
- [46] A. Jakalian, B. L. Bush, D. B. Jack, and C. I. Bayly. Fast, efficient generation of high-quality atomic charges. AM1-BCC model: I. Method. *J. Comput. Chem.*, 21(2):132–146, 2000.
- [47] A. Jakalian, D. B. Jack, and C. I. Bayly. Fast, efficient generation of high-quality atomic charges. AM1-BCC model: II. Parameterization and validation. *J. Comput. Chem.*, 23(16):1623–1641, 2002.
- [48] L. Belloni and I. Chikina. Efficient full newton-raphson technique for the solution of molecular integral equations - example of the spce water-like system. *Mol. Phys.*, 112(9-10):1246–1256, 2014.
- [49] P. Eastman and V. S. Pande. Efficient nonbonded interactions for molecular dynamics on a graphics processing unit. *J. Comput. Chem.*, 31(6):1268–1272, 2010.
- [50] P. Eastman and V. S. Pande. Constant constraint matrix approximation: A robust, parallelizable constraint method for molecular simulations. *J. Chem. Theory Comput.*, 6(2):434–437, 2010.
- [51] P. Eastman, M. S. Friedrichs, J. D. Chodera, R. J. Radmer, C. M. Bruns, J. P. Ku, K. A. Beauchamp, T. J. Lane, L.-P. Wang, D. Shukla, T. Tye, M. Houston, T. Stich, C. Klein, M. R. Shirts, and V. S. Pande. OpenMM 4: A reusable, extensible, hardware independent library for high performance molecular simulation. *J. Chem. Theory Comput.*, 9(1):461–469, 2013.
- [52] M. S. Friedrichs, P. Eastman, V. Vaidyanathan, M. Houston, S. Legrand, A. L. Beberg, D. L. Ensign, C. M. Bruns, and V. S. Pande. Accelerating molecular dynamic simulation on graphics processing units.

- J. Comput. Chem.*, 30(6):864–872, 2009.
- [53] M. R. Shirts, D. L. Mobley, J. D. Chodera, and V. S. Pande. Accurate and efficient corrections for missing dispersion interactions in molecular simulations. *J. Phys. Chem. B*, 111(45):13052–13063, 2007.
- [54] J. D. Chodera and M. R. Shirts. Replica exchange and expanded ensemble simulations as gibbs sampling: Simple improvements for enhanced mixing. *J. Chem. Phys.*, 135(19):194110, 2011.
- [55] A. Rizzi, P. B. Grinaway, D. L. Parton, M. R. Shirts, K. Wang, P. Eastman, M. Friedrichs, V. S. Pande, K. Branson, D. L. Mobley, and J. D. Chodera. Yank: A gpu-accelerated platform for alchemical free energy calculations.
- [56] A. Onufriev, D. Bashford, and D. A. Case. Exploring protein native states and large-scale conformational changes with a modified generalized born model. *Proteins*, 55(2):383–394, 2004.
- [57] J. L. Knight and C. L. Brooks. Surveying implicit solvent models for estimating small molecule absolute hydration free energies. *J. Comput. Chem.*, 32(13):2909–2923, 2011.
- [58] D. Borgis, R. Assaraf, B. Rotenberg, and R. Vuilleumier. Computation of pair distribution functions and three-dimensional densities with a reduced variance principle. *Mol. Phys.*, 111(22-23):3486–3492, 2013.
- [59] D. de las Heras and M. Schmidt. Better than counting: Density profiles from force sampling. *Phys. Rev. Lett.*, 120:218001, May 2018.